

## **NOTICE CONCERNING COPYRIGHT RESTRICTIONS**

This document may contain copyrighted materials. These materials have been made available for use in research, teaching, and private study, but may not be used for any commercial purpose. Users may not otherwise copy, reproduce, retransmit, distribute, publish, commercially exploit or otherwise transfer any material.

The copyright law of the United States (Title 17, United States Code) governs the making of photocopies or other reproductions of copyrighted material.

Under certain conditions specified in the law, libraries and archives are authorized to furnish a photocopy or other reproduction. One of these specific conditions is that the photocopy or reproduction is not to be "used for any purpose other than private study, scholarship, or research." If a user makes a request for, or later uses, a photocopy or reproduction for purposes in excess of "fair use," that user may be liable for copyright infringement.

This institution reserves the right to refuse to accept a copying order if, in its judgment, fulfillment of the order would involve violation of copyright law.

## Passive Seismic Monitoring of a Flow Test in the Salton Sea Geothermal Field

S. P. Jarpe, P. W. Kasameyer, and C. Johnston

Lawrence Livermore National Laboratory, Livermore, CA

### ABSTRACT

The purpose of this seismic monitoring project was to characterize in detail the micro-seismic activity related to the flow-injection test in the Salton Sea Geothermal Field. Our goal was to determine if any sources of seismic energy related to the test were observable at the surface, using both conventional seismic network techniques and relatively newer array techniques. These methods allowed us to detect and locate both impulsive microearthquakes and continuous sources of seismic energy.

Our network, which was sensitive enough to be triggered by magnitude 0.0 or larger events, found no impulsive microearthquakes in the vicinity of the flow test in the 8 month period before the test and only one event during the flow test. We have observed some continuous seismic noise sources that may have been caused by fluid flow at depth, but the amplitudes of these sources were not large enough to be unambiguously distinguished from surface sources.

### Introduction

Geothermal reservoirs often produce detectable geophysical signals both before and during production. These signals, if understood, could provide valuable information about the processes taking place within the reservoir. This kind of information can be used to guide reservoir development strategies. Some geophysical signals, such as resistivity and gravity, are well understood, and their contribution to reservoir engineering models has been demonstrated in many geothermal fields. Other geophysical signals, including seismic signals, are not so well understood. Lawrence Livermore National Laboratory (LLNL) has a program to collect case histories of surveys of geophysical signals produced during injection and production of geothermal fields. In this paper, we describe a case study of seismic signals produced during a small-scale injection-production test at the Salton Sea Geothermal Field.

Several different types of seismic signals have been observed in geothermal areas. Tectonic earthquakes associated with geothermal production have been observed at the Geysers Geothermal Field [Eberhart-Phillips and Oppenheimer, 1984]. Acoustic emissions (high-frequency microearthquakes) have been observed during hydraulic fracturing at Fenton Hill [Fehler and Barne, 1985], and during

reservoir production in Japan [Niitsuma et al., 1985]. Geothermal "noise" (anomalously high seismic signals having no clear onset and lasting longer than several tens of seconds) has been observed near several geothermal areas [Douze and Laster (1979), Goforth et al., (1972)].

The area where the flow test took place is in the transition between the Brawley seismic zone and the San Andreas Fault system. The Brawley Seismic zone is a broad area of moderate seismicity extending NNW from the Imperial Fault to the San Andreas Fault. For a discussion of the seismicity and tectonics of the region, see Nicholson et al., 1986.

The flow-injection test conducted as the second phase of the SSSDP provided an opportunity to study seismic signals associated with the initial fluid production from a well-studied area. During the first phase of the SSSDP, the State 2-14 well was drilled to a depth of 3 km. During the flow/injection test, fluids produced from an open section of State 2-14 between approximately 2000 m and 3200 m depth were injected into Imperial 1-13, about 600 m to the north (Fig. 1). The flow continued for approximately 30 days.

We installed a seismic recording system to monitor microearthquakes and continuous seismic noise signals associated with the initial production of these two wells. Our recording network and recording system was capable of detecting all types of events previously seen in geothermal fields, except for acoustic emissions with dominant frequencies greater than 30 Hz.

Our processing of the data collected during the flow test period using both network and array methods found no evidence of impulsive microearthquakes and no conclusive evidence of noise energy originating at depth in the flow test zone.

### Seismic Network Description

Figure 1 shows the configuration of the LLNL seismic stations during the flow test. Two sets of stations were deployed; seven three-component stations within a 3 km radius of the two wells, and three small (100 m aperture) arrays at distances of 1 to 2 km. The network of three-component stations, which provide primarily phase arrival times, were used to detect and locate microearthquakes in

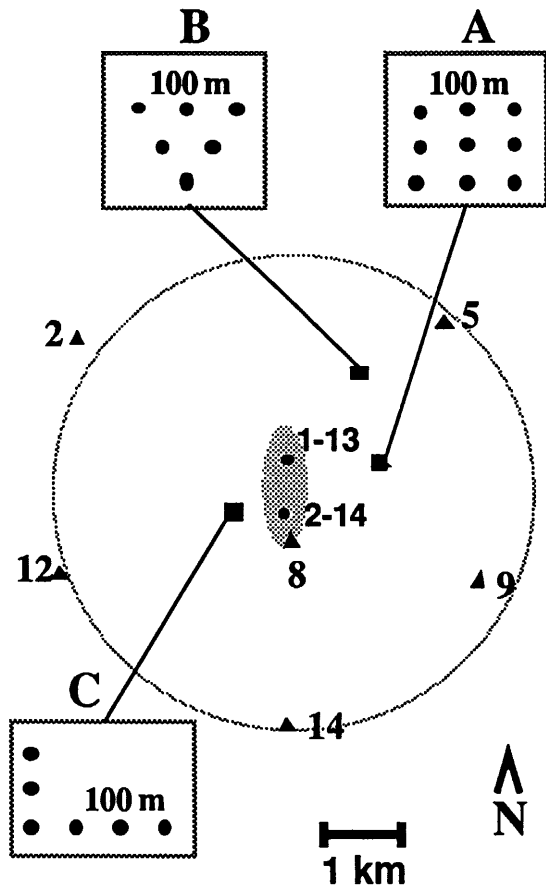


**Figure 1.** Map of the LLNL seismic network during the June, 1988 flow/injection test. The triangles are three-component station locations and the squares are the array locations. The insets show the geometries of the arrays. The shaded elliptical zone delineates the area within which we expected to see seismic activity related to the test.

the traditional manner. The arrays, which can provide direction, velocity, and depth information for any incoming seismic energy, were used to monitor all sources of seismic energy originating from the flow/injection zone.

The seismic signals were digitized at each station at a rate of 120 samples/sec and the digital signals transmitted to the central recording site located near well 2-14. The frequency range covered by the three-component stations was 1 to 30 Hz. The arrays were optimized for signals between 3 and 25 Hz. All of the sensors were buried several inches below the ground surface.

### Microearthquake Monitoring

To record impulsive microearthquakes, an event detection process at a central recording computer monitored all of the

signals continuously and archived all of the waveforms when a detection threshold was exceeded at the required number of stations. To characterize and locate the microearthquakes detected in this way, the arrival times of the direct P and S seismic phases were used in a standard least-squares inversion location algorithm.

We monitored the flow test zone for background seismicity between Sept. 1987 and the beginning of the flow test on June 2, 1988. During this time, the system operated in the event-detect mode. Although we had more than 1500 detections, no microearthquakes occurred within the flow test zone. Most of the earthquakes we recorded were associated with the Brawley seismic zone. Our earthquake locations indicated that many of these events were located just outside our network, however, and from the size of these events can estimate the lower detection threshold of our system to be magnitude 0.0.

Our examination of the data collected during the flow/injection test did not reveal any detectable (larger than M 0.0) microearthquakes within the zone of interest, except for one event that will be discussed in detail below. This negative result indicates that neither stress nor thermal effects of the flow test were large enough to induce microearthquakes during this shallow test.

### Comparison of traditional and array seismic methods

An array is a group of sensors arranged so that energy arriving at all of the sensors is coherent. This coherence can be exploited to cancel incoherent noise and obtain directional information about incoming signals. The desired arrangement of the sensors is dependent on the properties of the surface material and the frequency of signals expected. For our experiment, we designed our arrays to be sensitive to energy between 3 and 25 Hz. We deployed three separate arrays so that we could determine the location of energy sources in the flow test zone.

We will first compare the performance of the arrays and the standard 3-component seismic stations for the characterization of impulsive seismic sources. This will also provide a brief introduction to the methods used for processing array data. We will then describe how arrays can be used to characterize continuous seismic sources, or seismic noise.

When State 2-14 was first opened, we recorded a single small (magnitude -0.5) seismic event followed a few seconds later by an air wave. The cause of this signal is most likely a result of the initiation of fluid flow in the well column, but it provides us an opportunity to compare the monitoring capabilities provided by the traditional networks with the experimental array methods. We will present here in detail the information that we have been able to infer about these signals using both the seven station three-component network and the three arrays.

Three vertical component waveforms for the flow event

are plotted in Figure 2. The event-to-station distance is increasing from the top to the bottom trace. The seismic wave and the air wave are clearly differentiated by the difference in moveout across the network.

The same information can be obtained by computing the narrow band 2-dimensional wavenumber [Aki and Richards, 1980] from the signals at one of the arrays (array a). Figure 3 shows contour plots of power as a function of the narrow band 2-dimensional wavenumber for the air wave and the seismic phase. The azimuth of arrival is obtained from the azimuthal position of the peak power. The wavenumber of the arrival is obtained from the radial position of the peak. The apparent velocity is the ratio of the frequency at which the spectrum is calculated and the wavenumber.

It can be seen from Figure 3 that the two phases are arriving from the same azimuth, but that their apparent velocities are quite different. For the air wave, the frequency is 3 Hz and the peak wavenumber is 6.4 km<sup>-1</sup>, yielding a velocity of 0.33 km/sec., which is the velocity of sound.. For the seismic wave, the frequency is 8 Hz and the peak wavenumber is 3.48 km<sup>-1</sup> resulting in an apparent velocity of 2.3 km/sec.

We were able to locate this event using both the network and the three arrays. The seismic velocity structure used for the location was from Frith, (1978). The locations were similar using both methods (Figure 4.). The depths calculated from the network and the arrays were also similar (0.5 km).

For earthquake characterization and location, then, three arrays or six network stations can provide equivalent performance. There is no significant advantage to either configuration from an operational standpoint. The next section will demonstrate the advantages that the array methods provide for characterizing continuous sources of energy, or "noise".

### Noise Monitoring

Arrays are extremely useful for characterizing continuous noise sources associated with geothermal areas because they provide directional and depth information about seismic signals. This ability can be used to screen out noise from cultural sources, which are typically located at the surface.

The discrimination of surface and deep sources is done on the basis of phase velocity. Using known deep and shallow sources, we determined that surface sources had velocities less than 2 km/sec, and deep sources (> 0.5 km depth) had velocities greater than 2 km/sec.

The range of velocities resolvable at a given frequency is dependent on the size of the array. For our arrays, the energy with frequencies less than about 5 Hz is primarily surface energy, and frequencies greater than 20 Hz are primarily deep sources. We attempted to use this difference to monitor the noise originating in the deep part of the flow/injection zone.

For each of more than 900 twice-hourly 120 second data samples, we calculated the average noise power in a 60 deg. bearing range corresponding to the flow/injection zone at 4.5 Hz and 20 Hz. Figure 5 shows the results of this processing. The surface and deep noise power show an increase when the flow is greatest, suggesting that the the flow test is producing significant amounts of seismic energy. The high similarity of the surface and deep noise, however, indicates that the surface noise could be contaminating the 20 Hz signals.

The reason for this problem is that the arrays are too small and don't have enough elements to adequately filter out the large amplitude low-velocity signals from the much smaller deep signals. The overall amplitude of the 4.5 Hz power is approximately a factor of 10 greater than the 20 Hz power (Figure 5.), and any deep seismic sources that may be present are masked by the surface signal.

### Conclusions

Although we conducted an exhaustive search for earthquakes and continuous seismic energy related to the flow/injection test, we could not find any conclusive evidence for significant amounts of this energy.

Other sources of seismic energy not directly related to the flow test allowed us to explore the usefulness of seismic arrays for characterizing both continuous and impulsive sources of energy. Our results indicate that in a geothermal environment where significant levels of deep seismic energy are present, arrays can provide useful information not available from traditional seismic networks.

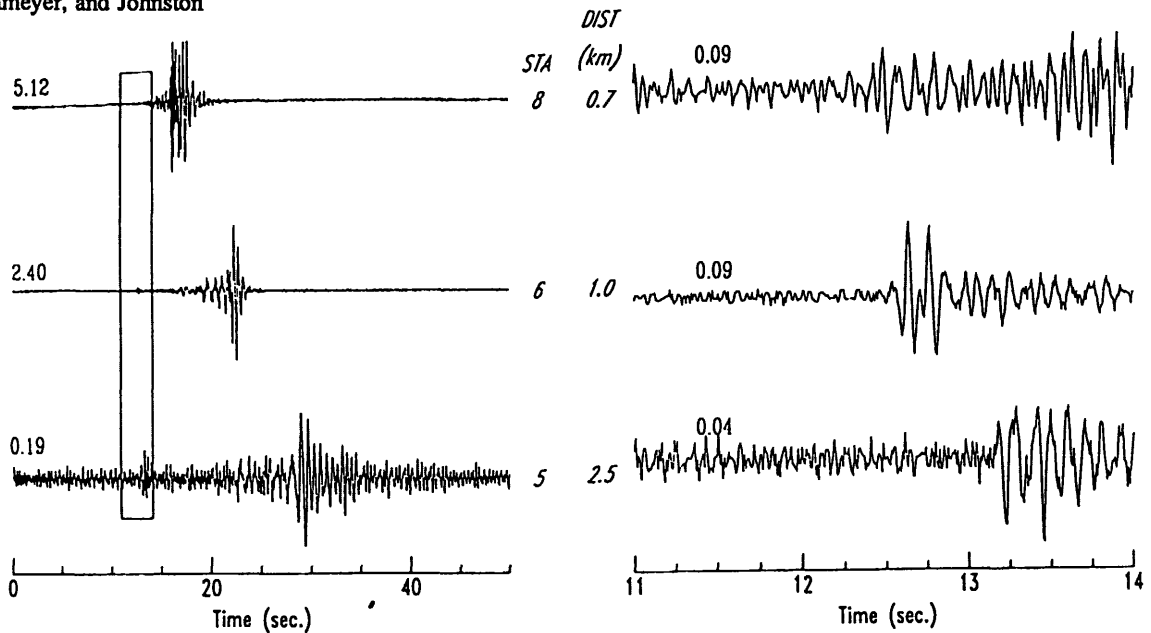


Figure 2. Seismograms from the flow event from stations at three different distances. At left is a 50 second segment dominated by the high-amplitude air wave. At right is the smaller seismic portion of the signal enclosed by the box in the left figure. Zero time is June 2, 1988 00:41:44, 10 minutes after State 2-14 was opened. The number above each trace is the maximum amplitude of the seismogram times  $10^{-4}$  nm/sec. The distance between the station and the event is shown between each pair of traces.

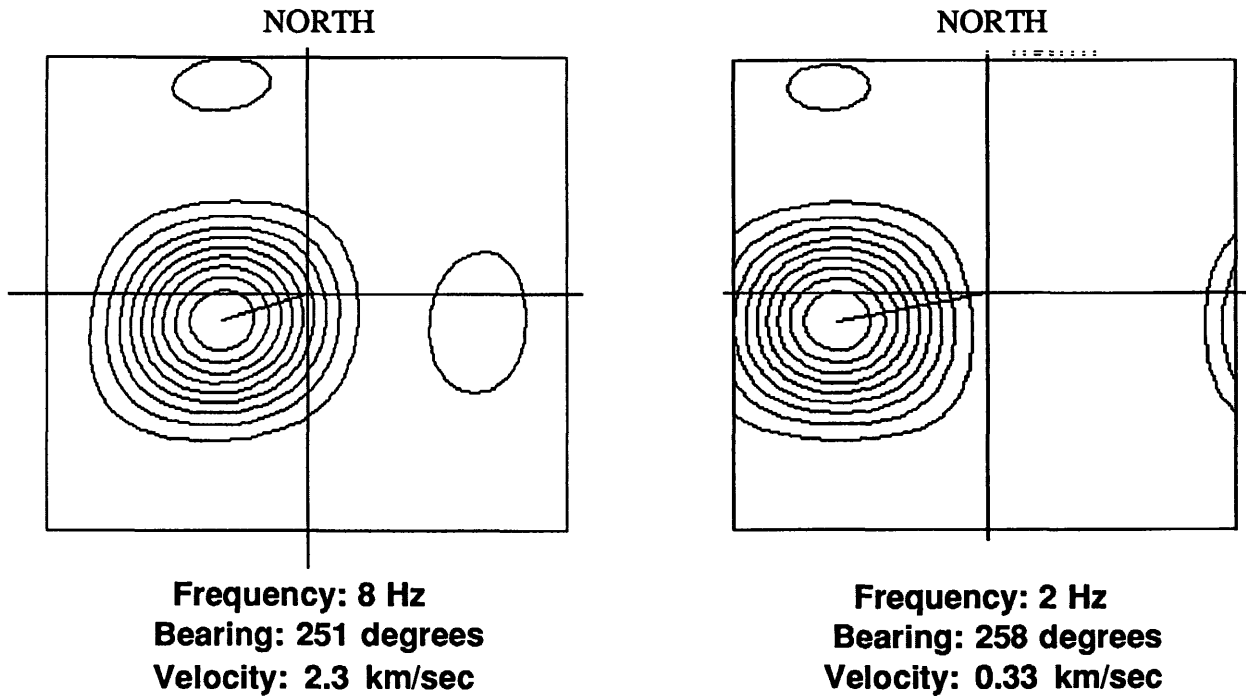
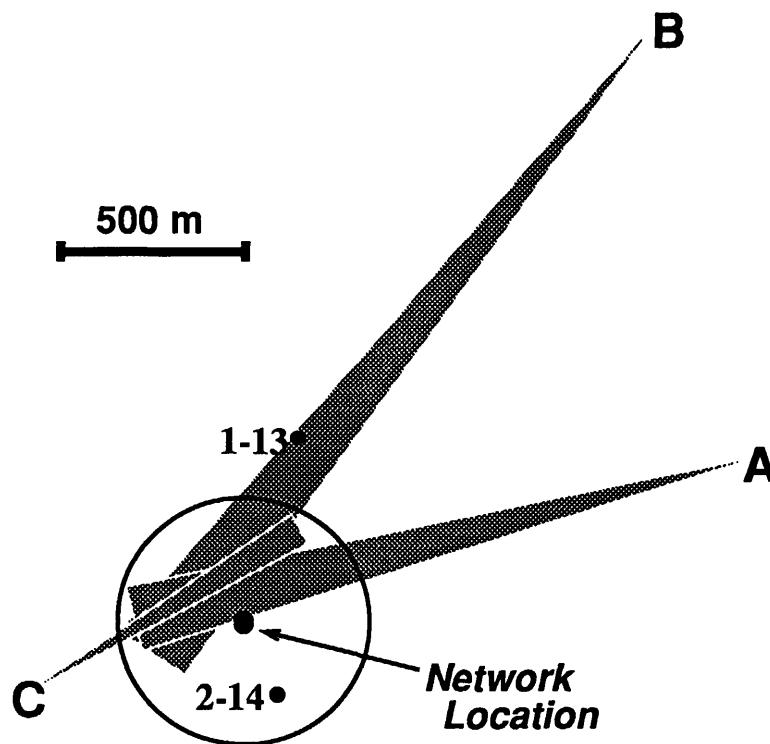


Figure 3. Contours of narrow-band 2-dimensional wavenumber power for the seismic (left) and air (right) waves recorded at array A. The bearing is measured clockwise from north. The wavenumber is  $0 \text{ km}^{-1}$  at the center and  $10 \text{ km}^{-1}$  at the edge of the plot.



**Figure 4.** Summary of location results for the seismic part of the flow event. The array location is defined by the intersection of the beams from the three arrays. The network location is obtained from the arrival times at the network stations. The uncertainty in the network location (400 m) is indicated by the circle centered on the location. The network and array locations are the same, within the uncertainties of each measurement.

### Acknowledgements

We would like to acknowledge the contributions of Don Rock and Dan Ewert to the fielding of the seismic network. Unocal Geothermal Division and Kennecott-Australia Exploration Ltd. provided instrument sites. Bechtel Corporation provided support at the recording site. This work was performed under the auspices of the U.S. Department of Energy by the Lawrence Livermore National Laboratory under Contract W-7405-Eng-48. Funding was provided by the Reservoir Technology Program of Department of Energy Geothermal Technology Division.

### References

- Aki, K., and P. G. Richards (1980). *Quantitative Seismology: Theory and Methods*, (Volume 2) ch. 11, sec. 4.
- Eberhart-Phillips, D., and D. H. Oppenheimer, (1984). Induced Seismicity in the Geysers Geothermal Area, California, *Journal of Geophysical Research* 89, 1191-1207.
- Frith, R. B. (1978). A Seismic refraction investigation of the Salton Sea Geothermal Area, Imperial Valley, California, (Master's thesis, U. C. Riverside)
- Goforth, T. T., E. J. Douze, and G. G. Sorrells, (1972). Seismic noise measurements in a geothermal area, *Geophysical Prospecting* 20, 76-82.
- Douze, E. J., and S. J. Laster, (1979). Seismic array noise studies at Roosevelt Hot Springs, Utah geothermal area, *Geophysics* 44 1570-1583.
- Nicholson, C., L. Seeber, P. Williams, and L. Sykes (1986). Seismic evidence for conjugate slip and block rotation within the San Andreas Fault system, southern California, *Tectonics* 5, 629-48.
- Niitsuma, H., K. Nakatsuka, N. Chubachi, H. Yokoyama, and M. Takanohashi (1985). Acoustic emission measurement of geothermal reservoir cracks in Takinoue (Kakkonda) field, Japan, *Geothermics* 14, 525-538.

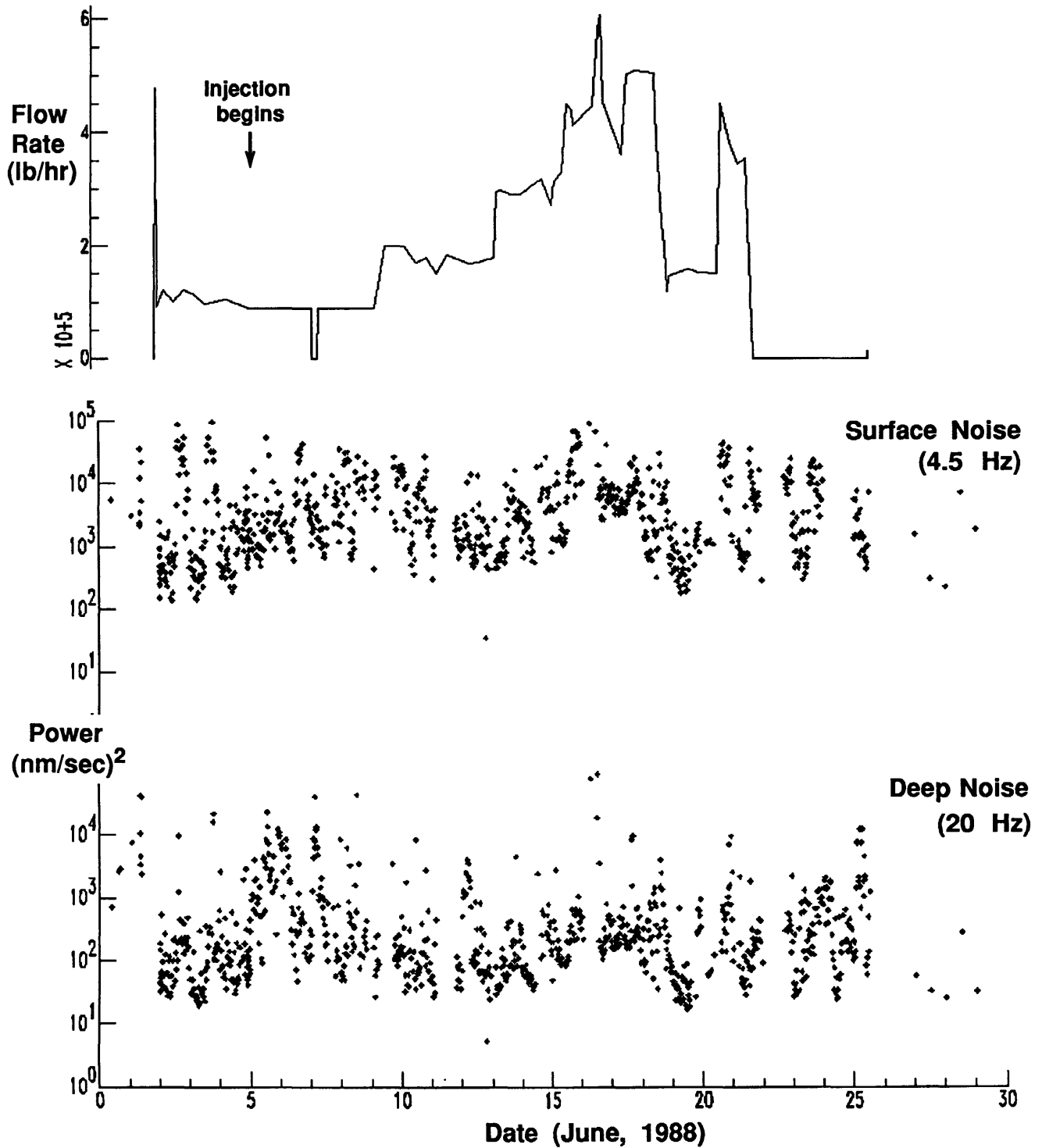


**Figure 5.** Flow rate (top) and surface and deep noise power at array a as a function of time during the entire flow test. The power for each time segment was obtained by integrating the power as a function of bearing over a 60 deg. range corresponding to the flow/injection zone (see Figure 1.). At a frequency 4.5 Hz, the seismic energy is limited to surface sources, and at 20 Hz, the seismic energy should be primarily from deep sources.